Joanna Hucińska
Faculty of Mechanical Engineering, Technical University of Gdańsk, Poland

SULPHIDE CORROSION PRODUCTS IN CARBON STEEL AFTER PROLONGED SERVICE IN LOW-SULPHUR REFINERY ENVIRONMENT

ABSTRACT

Characteristics of sulphide corrosion products in K18 carbon steel after 11 years of service in a low-sulphur refinery furnace environment have been examined in order to better understand the mechanism of sulphur-related damage to the steel. Optical microscope and scanning/transmission electron microscopes techniques have been involved in the study. Four types of the corrosion products of different morphology and origin have been presented: (1) iron sulphide scale on the steel surface, (2) sulphur-rich particles at ferrite grain boundaries, (3) degraded sulphur-enriched cementite particles at other ferrite grain boundaries and similar particles within pearlite grains, and (4) irregular iron sulphide inclusions in the subsurface metal layer that were not-related to the boundaries of the grains.

INTRODUCTION

Sulphur and its compounds are common corrosive contaminants encountered in high temperature refinery environments. The destructive action of sulphur on the metal alloys has been known for many years, and extensive researches have been carried out to establish the mechanism of high temperature sulphide corrosion and to work out protection methods to be used [1-6]. Numerous studies have been performed to predict the relative corrosivity of various refinery streams and to select materials with respect to sulphide corrosion resistance [1-6]. Morphology, chemistry, structure and properties of sulphide scales have also been thoroughly examined [4,5].

However, the understanding of the mechanism of sulphide corrosion is still unsatisfactory. Studies of the corrosion product features may greatly contribute to the solution to this complex phenomenon. New testing techniques that are available now allow for much more detailed characteristics of the sulphide corrosion products than those used in the past. In the present work characteristics of sulphide scale and internal sulphur-rich precipitates formed in a carbon steel during long-term service in a low sulphur refinery furnace environment have been examined. Atraditional optical microscope and modern electron microscopes equipped with X-ray energy dispersive spectrometers (EDS) have been involved in the study.

EXPERIMENTAL

The material used for the studies was a commercial carbon steel. The steel was in form of a tube of 168 mm diameter, and 7 mm thickness. The tube was in use in the refinery furnace for 11 years. The characteristics of the steel and the service conditions are shown in Table 1.

Table 1. *Characteristics of the steel tested and the service conditions*

Characteristics	Description
Composition in wt. %	C–0.17, Mn–0.69, Si–0.22, P–0.035, S-0.035, Cr-0.11, Ni-0.10, Cu-0.17
Grade	K18 under specifications of PN-75/H-84024 (Polish Standard)
Heat treatment of steel	Normalising
Equipment	Furnace in desulphurising unit
Environment	Naphtha after desulphurisation, about 0.3 ppm of sulphur. Temperature and pressure: 200-220°C, 140 kP (first 9 years) and 130-160°C, 60 kP (last 2 years)
Max. metal skin temperature	About 380°C (first 9 years) and about 220°C (last 2 years)

Some full-section samples of maximum metal skin temperature situated on the fire side of the furnace chamber were collected from the tube. They were compared with a sample from an as-received tube. Plane orthogonal sections of the samples were prepared metallographically. They were etched using a solution of 4% by volume of nitric acid in ethanol and examined making use of a Neophot 32 optical microscope (OM), and scanning electron microscopes (SEM) linked with the EDS: a field emission Hitachi 4200 SEM and a Philips XL 30E SEM.

Carbon extraction replicas were prepared from polished and etched sections taken from the as-received and the ex-service specimens. The electropolishing was performed in a solution of 10% by volume of perchloric acid in glacial acetic acid at 35-40 V, followed by etching in a solution of 1.5% by volume of perchloric acid and 2% by volume of nitric acid in ethanol at 4 V. The sections were vacuum covered with a film of carbon of 100-200 nm thickness, which was removed by electrolytic etching at 10-15 V in the solution of perchloric and nitric acids in ethanol, and collected on preparation grids for transmission electron microscope (TEM) examinations. The extracted precipitates/particles were identified in a Jeol JEM 100C TEM using a selective diffraction technique, while their chemical composition was analysed by use of the EDS. The composition of single particles at boundaries of ferrite grains and groups of particles in pearlite grains was examined using electron beams of diameters adjusted to the particles.

RESULTS

SEM examinations

In Figs. 1(a)-(d) through 2, 3(a),(b) the SEM micrographs of the sulphur-attacked steel surface, i.e. the inside surface (IS) of the tube are presented. In Fig. 1(a) a crumbled, multi-layer scale on the surface is shown, and the chemical composition of some iron/sulphur-rich layers of the scale in an open shallow pit is described in Fig. 1(b). Non-uniform progress of metal losses on the steel surface due to sulphide corrosion is indicated by pits situated on the surface: the open pits in Figs. 1(a)-(c), and the closed pit in Fig. 1(d). It can be seen that the sulphide corrosion preferentially proceeded along the boundaries of the ferrite grains and across the pearlite grains. This is marked by the sulphide scale penetrating the boundaries of the ferrite grains to a greater depth than the insides of these grains in Figs. 1(b)-(d), and the scale developing through the pearlite grains in Fig. 1c and Fig. 2. The latter micrograph was taken about 0.05 mm beneath the steel surface.

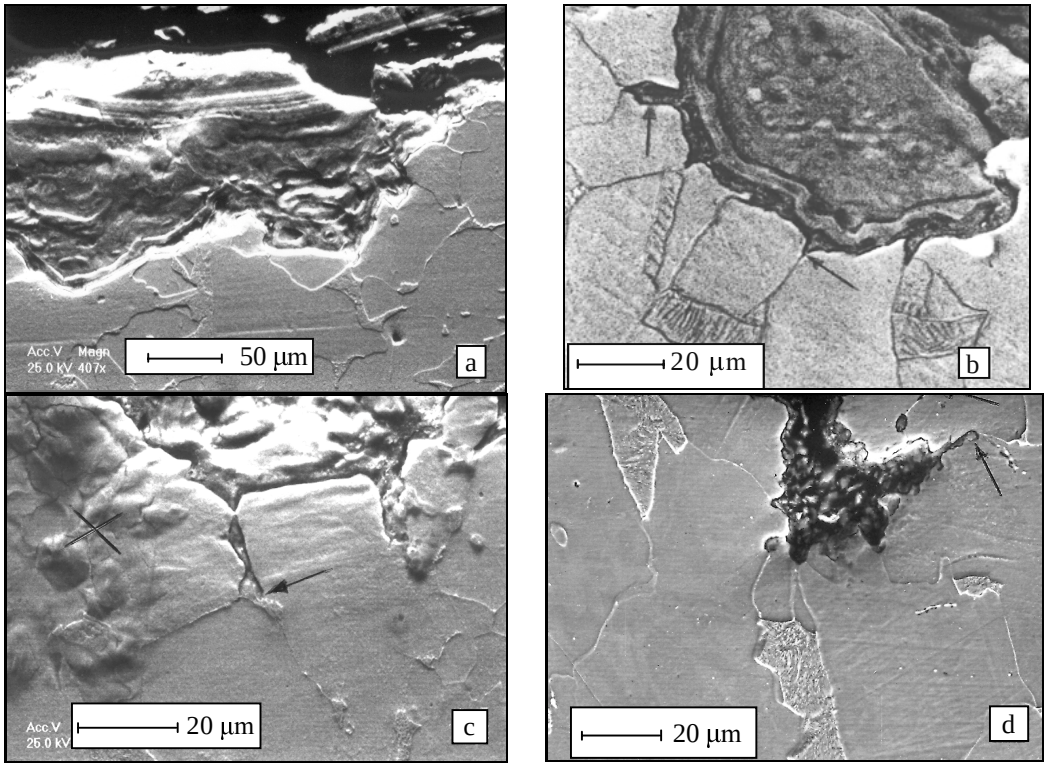

Fig. 1. SEM micrographs of the cross sections of the sulphur-attacked carbon steel showing iron sulphide scale on the steel surface of chemical composition (in wt. %) indicated in (b): Fe-82.55, S-17.45 (1), Fe-71.40, S-28.60 (2), Fe-79.46, S-20.54 (3) (EDS). The open pits on the surface (a-c) and the closed pit (d) are presented. Sulphide corrosion progress along ferrite grain boundaries (b, d) and through the perlite grain (c) is indicated by arrows.
The centre of the brittle fracture area is marked by a cross

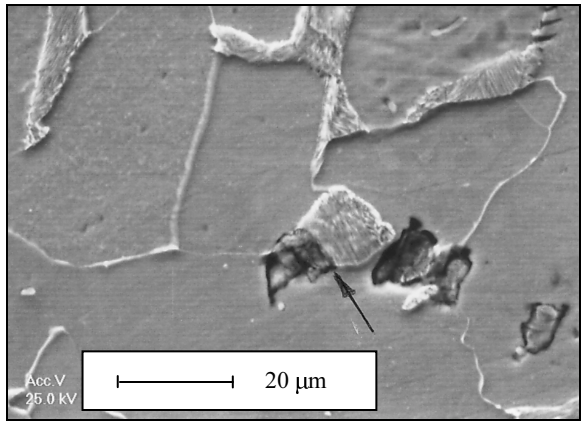

Fig. 2. A SEM micrograph of the cross-section of the sulphur-attacked carbon steel illustrating iron sulphide inclusions about 0.05 mm beneath the steel surface. Sulphide corrosion progress through the perlite grain is indicated by an arrow

Figs. 3(a), (b) illustrate a mode of damage to the steel at an advanced stage of the sulphur attack when there were no longer pearlite grains in the subsurface metal layer and some ferrite grain boundaries disappeared. In this ferrite matrix area irregular iron sulphide inclusions formed. Conglomerations of the inclusions weakened the strength of the subsurface layer to such a degree that some parts of the layer fall off.

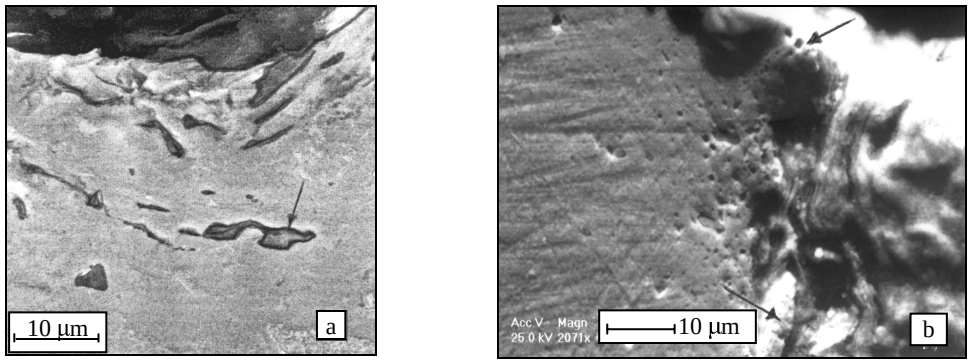

Fig. 3. SEM micrographs of the cross sections of the sulphur-attacked carbon steel showing irregular iron sulphide inclusions beneath the steel surface. In (a) the inclusion of chemical composition: Fe-80.05 wt. %, S-19.95 wt. % is indicated by an arrow. In (b) impaired steel particles separating from the surface are indicated

The SEM examinations revealed that the scale formed on the carbon steel under investigation contained both the sulphide corrosion products and the mechanically separated steel particles. It is evident in Fig. 3(b) that at the advanced stage of the corrosion the ductile-mode failure of the subsurface layer developed, while at the earlier stage in Fig. 1(d) some brittle fracture prevailed.

OM examinations

In some areas beneath the surface continuous layers of an internal iron sulphide scale formed. The internal scale probably developed due to the growth and the linking of the subsurface pits and the irregular iron sulphide inclusions in the subsurface area. A part of the scale that was recorded using optical microscope is presented in Fig. 4. The microstructure of the steel showing white ferrite grains and black pearlite grains can be seen. The parts of the material close to the both edges of the scale were decarburized that is evidenced by an increased amount of the ferrite grains at the expense of the pearlite grains.

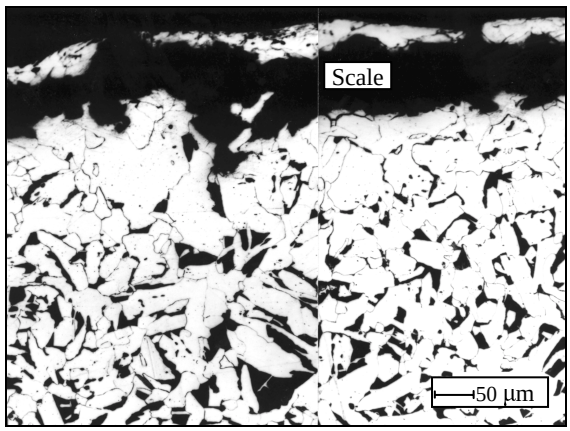

Fig. 4. An OM micrograph of the cross sections of the sulphur- attacked carbon steel showing internal sulphide scale. Decarburization of the steel close to the scale is evidenced by the increased amount of white ferrite grains at the expense of black pearlite grains

TEM examinations

Fig. 5 shows a TEM micrograph of the carbon extraction replica of the as-received carbon steel. Cementite lamellae within a pearlite grain are presented. The diffraction analysis confirmed that they were of Fe_3C type. According to EDS analysis the lamellae contained mainly iron, and small amounts of sulphur and tramp elements, such as manganese, chromium, silicon (Table 2).

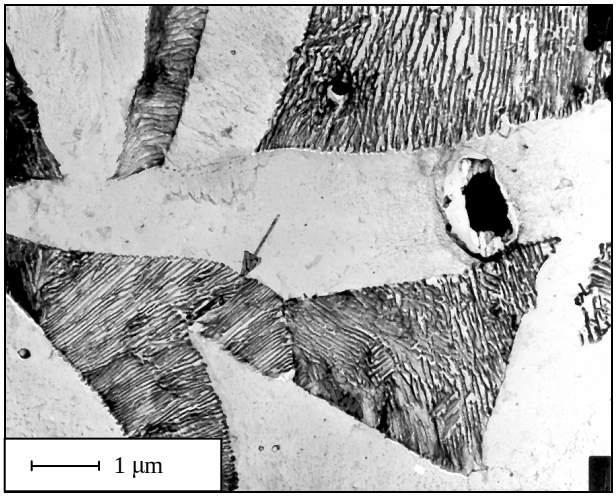

Fig. 5. Fig. 4. A TEM micrograph of the carbon extraction replica of the as-received carbon steel showing cementite lamellae within a pearlite grain

Table 2. *Chemical composition of cementite lamellae within pearlite grains in the as-received carbon steel (TEM, EDS)*

Chemical composition in wt. %				
Fe	Mn	Cr	Si	S
97.4 ± 0.57	1.41± 0.21	0.17± 0.10	0.32± 0.08	0.36± 0.15

TEM/EDS examinations of the ex-service carbon steel revealed that a remarkable degradation of cementite took place under the influence of the sulphur. The results of the EDS analyses shown in Table 3 indicate that big amounts of sulphur were present in the degraded particles situated beneath the IS of the tube and down to a depth of 3.5 mm. The greatest concentration of sulphur was found at 0.2 mm beneath the surface and the concentration gradually decreased towards the middle-wall. The degraded particles were also enriched in tramp elements: manganese, chromium and silicon. The diffraction analysis of the degraded particles indicated their heavily deformed quasi-crystalline structure. In Fig. 6 an example of some degraded precipitates within a pearlite grain are presented. Some damage to lamellar microstructure of cementite and a partial disintegration of the pearlite grain may be seen. A total disintegration of the sulphur-attacked grains resulted in formation of a decarburized layer beneath the surface that was presented in Figs. 3, 4.

Table 3. *Chemical composition of degraded precipitates within pearlite grains in the ex-service carbon steel (TEM, EDS)*

Distance from the IS in mm	Number of grains	Chemical composition in wt. **%:** variation range **/** average				
		Fe	Mn	Cr	Si	S
0.2	21	53.52-92.98 **80.57**	0.00-16.39 **2.78**	0.00-11.37 **3.76**	0.00-9.49 **2.81**	1.42-26.97 **10.07**
0.8	18	71.76-96.92 **87.92**	0.00-9.59 **1.71**	0.00-9.50 **2.51**	0.00-7.45 **2.33**	0.44-12.17 **5.53**
1.5	16	84.38-97.82 **92.90**	0.00-2.94 **1.18**	0.00-3.02 **0.95**	0.00-8.57 **2.66**	1.01-5.97 **2.31**
2.5	25	93.90-99.73 **97.02**	0.00-3.48 **1.28**	0.00-1.84 **0.44**	0.00-0.48 **0.07**	0.10-3.03 **1.19**
3.5	12	91.96-98.57 **97.01**	0.72-1.63 **1.17**	0.25-2.00 **0.69**	0.04-2.33 **0.48**	0.00-3.16 **0.65**

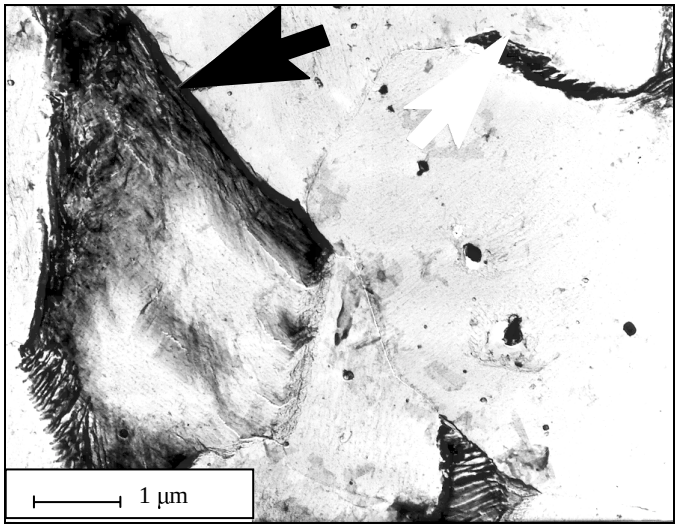

Fig. 6. A TEM micrograph of the carbon extraction replica of the ex-service carbon steel showing degraded cementite precipitates within the pearlite grain (black arrow) and at the boundary of ferrite grains (white arrow)

TEM/EDS examinations of ferrite grain boundaries revealed the presence of long and thin, isolated inclusions (Fig. 6). The greatest concentration of the precipitates was found close to the steel surface. Their composition was more differentiated than the composition of the pearlite--related particles. There were precipitates similar to the former and particles containing sulphur mainly; one precipitate similar to manganese sulphide was also recorded (Table 4).

Table 4. *Chemical composition of 8 following precipitates situated at ferrite grain boundaries 0.2 mm beneath the surface of the ex-service steel (TEM, EDS)*

Grain	Chemical composition in wt. %					Grain	Chemical composition in wt. %				
No.	Fe	Mn	Cr	Si	S	No.	Fe	Mn	Cr	Si	S
1	4.11	36.44	0.49	0.00	58.96	5	74.12	10.16	0.00	10.27	5.44
2	2.96	0.66	0.52	0.28	95.59	6	88.03	3.49	0.00	3.13	5.35
3	86.47	1.97	3.65	2.56	5.35	7	7.83	0.10	0.36	0.00	91.71
4	1.26	12.30	0.00	0.04	86.40	8	72.25	0.00	11.83	0.00	15.92

SUMMARY

Characteristics of sulphide corrosion products in K18 carbon steel after 11 years of service in the refinery furnace environment, which contained about 0.3 ppm of sulphur, have been examined by means of the optical microscope technique and the scanning/transmission electron microscope techniques.

Despite of the low sulphur content in the environment, a remarkable damage to the steel took place. The corrosion products formed on the steel surface and beneath the surface, down to the depth of 3.5 mm. Four types of the products of different morphology were revealed:

1. **Iron sulphide scale on the surface penetrating the inside of the steel along ferrite grain boundaries and across pearlite grains.** The scale was composed of particles originating from chemical reactions between sulphur and iron. At an advanced stage of the attack the scale also contained some mechanically separated steel particles.
2. **Unstable sulphur and tramp elements-enriched precipitates.** They originated from cementite precipitates situated within pearlite grains and along ferrite grain boundaries, which were destroyed due to diffusion of sulphur along the grain boundaries and interfacial ferrite/cementite boundaries. The greatest average concentration of sulphur in the precipitates, of about 10 wt. %, was recorded close to the surface. The concentration gradually decreased towards the steel inside reaching 0.65 wt. % at 3.5 mm beneath the surface.
3. **Ferrite grain boundary particles containing more than about 85 wt. % of sulphur.** The presence of these particles may be linked with the sulphur penetrating free of cementite boundaries of ferrite grains.
4. **Irregular iron sulphide inclusions in the subsurface grain boundary-free metal layer.** The inclusions formed after the cementite in the layer had been destroyed.

The in-service impairments of the steel presented in the paper were due to the sulphur action only. This was because there were no other high temperature corrosion agents in the environment. Moreover, due to a relatively low temperature of the steel during the service, ranging from about 220-160˚C at the sulphr-attacked surface to 380-220˚C on the other surface, elevated temperature damage to the steel, which could be connected with impurity/tramp element segregation and cementite transformations, was excluded.

REFERENCES

1. Gutzeit J., in: *Process industry corrosion – the theory and practice.* NACE, Houston, 1986.
2. Couper A.S., Gorman J.W.: *Computer correlations to estimate high temperature H_2S corrosion in refinery streams.* Materials Protection and Performance 10 (1971), pp. 31-37.
3. Lai G.Y.: *High-temperature corrosion of engineering alloys.* ASM Int., Materials Park, OH, 1997.
4. McCoy J.D.: *Corrosion rates for H_2S at elevated temperatures in refinery hydrodesulfurization processes.* Materials Performance 13 (1974), pp. 19 -25.
5. McCoy J.D., Hamel F.B.: *Effect of hydrodesulfurizing process variables on corrosion rates.* Materials Protection and Performance 10 (1971), pp. 17-22.
6. Couper A.S.: *High temperature mercaptan corrosion of steel.* Corrosion 19 (1963), pp. 396t-401t.